Biochimica et Biophysica Acta, 1021 (1990) 182–190
Elsevier

BBAMEM 74709

Membrane–membrane interactions: parallel membranes or patterned discrete contacts

H. Darmani and W.T. Coakley

Microbial and Molecular Biology, School of Pure and Applied Biology, University of Wales College of Cardiff, Cardiff (U.K.)

(Received 20 July 1989)

Key words: Membrane–membrane interaction; Membrane surface properties; Erythrocyte adhesion; Cell adhesion; Interfacial instability

Theoretical and experimental studies of thin liquid films show that, under certain conditions, the film thickness can undergo a sudden transition which gives a stable narrower film or ends in film rupture at spatially periodic points. Theoretical analysis have also indicated that similar transitions might arise in the thin aqueous layer separating interacting membranes. Experiments described here show spatially periodic intermembrane contact points and suggest that spontaneous rapid growth of fluctuations can occur on an intermembrane water layer. Normal and pronase pretreated erythrocytes were exposed to 2% Dextran (450000 M_r) and the resultant aggregates were examined by light and transmission electron microscopy. Cell electrophoresis measurements were used as an index of pronase modification of the glycocalyx. Erythrocytes exposed to dextran revealed a uniform intercellular separation of parallel membranes. This equilibrium between attractive and repulsive intermembrane forces is consistent with the established Derjaguin, Landau, Verwey, Overbeek (DLVO) model for colloidal particle interaction. In contrast to the above uniform separation a spatial pattern of discrete contact regions was observed in cells coming together in dextran following pronase pretreatment. The lateral contact separation distance was 3.0 μm for mild pronase pretreatment and decreased to 0.85 μm for more extensive pronase pretreatments. The system examined here is seen as a useful experimental model in which to study the principles involved in producing either uniform separation or point contacts between interacting membranes.

Introduction

It was pointed out a number of years ago [1], and still remains largely true, that while the static forces (equilibrium of attractive and repulsive forces) involved in membrane fusion and adhesion have been studied extensively less attention has been given to the dynamic processes (membrane movements, due to net attractive intermembrane forces, which can influence the final form of the membrane-membrane contact) involved. Many studies in the area of bubble and of drop approach and coalescence have shown that the behaviour of the intervening liquid films and the properties of the interface strongly influence the outcome of the interactions [1]. Specifically, a film thinning under the influence of a net attractive pressure may reach a 'transition thickness' at which thickness fluctuations of the thin film grow spontaneously leading either to rupture of the thin film at spatially periodic points or to formation of a film with smaller thickness (as in black film formation [2–4]). Developing of such fluctuations on the narrowing water layer between approaching membranes might result in either (i) a small, essentially uniform separation, which may be described by modern extension [5,6] of the classical Derjaguin, Landau, Verwey and Overbeek (DLVO) theory of colloidal stability [7] or (ii) rupture of the aqueous layer to give spatially (not temporally) periodic contacts. By substituting published estimates of membrane constants into established thin film instability criteria Dimitrov [1] showed that spontaneous growth of thickness fluctuation might reasonably be expected on the thin aqueous layer between membranes which are moving towards each other. The stability of the thin film depends on the surface properties (e.g., surface tension and bending elasticity) of the interfaces between the thin film bulk phase and the surrounding bulk phases and on the normal interactions between the interfaces. The condition (a function of interfacial properties and

Correspondence: W.T. Coakley, Microbial and Molecular Biology, School of Pure and Applied Biology, University of Wales College of Cardiff, Museum Avenue, Cardiff CF1 3TL, U.K.

normal interactions) for spontaneous rupture of a non-thinning inter-membrane aqueous layer is not very different from those of a thinning inter-membrane water layer [1,8] while analysis of the latter situation has provided goof physical insight to the rupture process. We will use the stability condition for a non-thinning film for guidance in the present paper while recognising, where appropriate, that the aqueous film between cells thins as the cells come together. Prevost, Gallez and Sanfeld [9] have developed a stability analysis for a nonsymmetrical non-thinning film. New interaction terms (in addition to van der Waals forces) involving charge, repulsive hydration [10,11] and macromolecular cross-linking [12] have been introduced to analysis of the stability of an intermembrane aqueous layer.

While accepting, from theoretical predictions, that rupture of an intermembrane thin film could occur Dimitrov [1] remarked that the most serious problem for the theory was the lack of experimental data obtained in rigourously defined conditions about the basic result, the possibility for instability and rupture of the liquid film between membranes. Fisher, Parker and Haydon [13], in an interferometric study of lipid bilayer interactions across an aqueous layer, reported the first [14] measurement of the layer thickness (28 nm) at which rupture of a draining intermembrane film occurred. The film collapse was complete in less than the 10 ms resolution time of the experimental system and it was not possible to visualise wave growth or measure wavelength in that system.

Recent studies of polycation (polylysine and polyarginine [15,16]) and lectin (wheat germ agglutinin [17]) induced adhesion of erythrocytes showed that cell adhesion occurred by production of spatially periodic contact areas separated by average lateral distances of about 0.8 μm. The production of patterns of discrete contact regions was attributed to the breakup of the intercellular water layer as an interfacial instability (option(ii) in paragraph 1 above). In contrast, the membranes of erythrocyte clumps formed in 3% or 4% of 75000 M_r dextran [18,19] or in 2% w/v of 450000 M_r dextran [20] maintained a continuous parallel-membrane seam without detectable periodic interruption (consistent with option (i) in paragraph 1 above). However, a preliminary result [20] has shown that contact in 450000 M_r dextran gives a spatially periodic pattern if cells are pretreated with pronase.

In the present paper we report how the properties of the membrane surface determine whether adhesion results in a parallel-membrane situation or in spatially periodic contacts.

Materials and Methods

Erythrocyte suspension. Human erythrocytes were obtained by finger puncture into phosphate-buffered saline (PBS) containing 145 mM NaCl and 5 mM phosphate at pH 7.32. The cells were washed three times by centrifugation at $1200 \times g$ for 1 min and finally resuspended in PBS containing 0.2 mg $\cdot$ ml^{-1} bovine serum albumin (BSA; Sigma Ltd.). The cell concentration was determined using a haemocytometer and was adjusted by adding PBS so that it was in the range $(3–3.5) \cdot 10^7$ cells per ml.

Pronase pretreatment. 1 ml of the erythrocyte suspension was added to an equal volume of 1 mg $\cdot$ ml^{-1} pronase (Boehringer Mannheim GmbH) solution in PBS. The cells were exposed to pronase for a known time at room temperature and then centrifuged at $1200 \times g$ for 1 min. The cells were resuspended in 1 ml PBS containing BSA (0.5 mg $\cdot$ ml^{-1}).

Exposure to polymers. 0.5 ml of the erythrocyte suspension was added to an equal volume of PBS containing 4% Dextran T500 (M_r 450000, Sigma Ltd.) or 10 μg $\cdot$ ml^{-1} polylysine (M_r 275000, Sigma Ltd.). The resulting cell suspension was held at room temperature, with occasional shaking, for 30 min (dextran) or 10 min (polylysine) before fixation (when required) with an equal volume of glutaraldehyde (6% v/v, unless otherwise stated) in PBS.

Light microscopy. Following exposure to dextran or to polylysine cells in suspension were loaded, by capillarity, into 5 cm long 100 μm pathlength rectangular cross-section microslides (Camlab Ltd.) and examined by light microscopy. To improve contrast in the examination of the contact seam the field diaphragm of the Nachet 400 Research microscope was stepped down to about 20% of the maximum field width compared with the more usual value of 85%. Differential interference contrast microscopy was used routinely but the patterns could also be seen by conventional bright field microscopy.

Transmission electron microscopy. Cells (1 ml) which had been fixed following exposure to 2% dextran were immediately centrifuged at 1200 g for 1 min and resuspended in 1 ml buffer containing 3% glutaraldehyde. Following 30 min exposure at 4°C the cells were centrifuged at $1200 \times g$ for 1 min and resuspended in 1 ml 0.1 M cacodylate buffer (pH 7.4). The cells were washed twice at $1200 \times g$ for 1 min in cacodylate buffer. The cells were resuspended in 0.1% w/v osmium tetroxide in cacodylate buffer (pH 7.4) and left at 4°C for 1 h and then centrifuged at $1200 \times g$ for 1 min. The cells were then dehydrated by exposure to a graded series (50,70,80,95,100,100%) of ethanol. The dehydrated cells were resuspended in pure propylene oxide for 10 min and centrifuged at $1200 \times g$ for 1 min. This process was repeated for another 10 min exposure time and the centrifuged cells were finally resuspended in a 1:1 propylene-oxide/Epon-812 mixture (12.5 g Epon 812, 8 g dodecenyl succinic anhydride, 5.25 g Nadic methyl anhydride and 0.25 g 2,4,6-tridimethylamino methyl

phenol). The cells were then centrifuged at 1200 × *g* for 1 min and resuspended in pure Epon and left at 60 °C for 24 h.

Electrophoretic mobility. The cell suspension was diluted in PBS/BSA to approximately $1 \cdot 10^7$ cells/ml. 1 ml of the resulting suspension was further diluted by addition of 9 ml of 14.5 mM NaCl, 5 mM phosphate, 280 mM erythritol (pH 7.32). The electrophoretic mobility of cells in suspension was determined from velocity measurements of individual cells under the influence of an electric field in a particle micro-electrophoresis apparatus MK 11 (Rank Brothers, Botisham, Cambridge). The mobility of at least ten cells was determined for each enzymically pretreated sample and an average calculated. Electrophoretic mobilities were measured for each sample on which quantitative measures of lateral contact point separation were made.

Real time video-microscopy of adhesion. A light microscope and videosystem as described elsewhere [21] was used to follow the process of erythrocyte adhesion by dextran. A microscope was turned through 90 ° onto its back. An equal volume of control cells or of pronase (1 mg/ml initial concentration; 60 min) pretreated cells was added to a 4% dextran solution. 1.0 ml aliquot of the resulting cell suspension was added to a 1 cm high cuvette which was mounted on the vertical microscope stage. A 5-cm long 200 μm pathlength rectangular cross-section microslide (Camlab Ltd.) was placed, vertically, in the solution. Cell suspension was drawn into the microcapillary by capillarity. The process of cell-cell adhesion was then observed and recorded by video-microscopy using the ×40 objective.

Results

The mobility of cells in the cytophorimeter is expressed in Fig. 1, for different durations of pronase pretreatment, as a percentage of the mobility of control cells. Pronase caused a rapid decrease in electrophoretic mobility during the early minutes of exposure. The cell velocity had fallen to 54% of control values after 5 min and only decreased to 45% over the following 115 min. The limiting value of 45% of control mobility is similar to published values (35% for chymotrypsin, 40% for trypsin) for the effect of other proteinases on erythrocytes [22]. The percentage of control cell mobility remaining (PR) is used below as an index of the effect of pronase pretreatment of the cells. The use of this index is not intended to imply that charge depletion was the only, or even the most significant, cause of the observed effects.

Light micrographs of erythrocytes which had been fixed with glutaraldehyde following exposure to 2% dextran (final concentration) for 30 min at room temperature are shown in row (i) of Fig. 2. The clump of control cells in Fig. 2(i) shows the convex-ended form

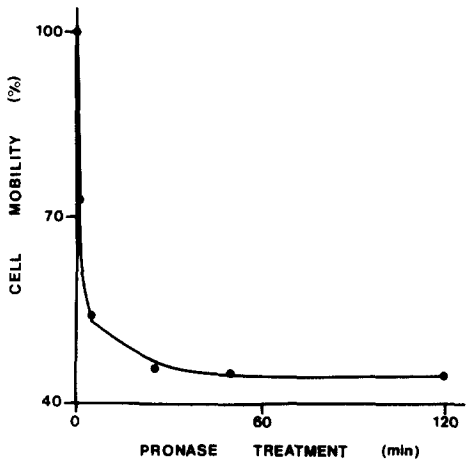

Fig. 1. Cell mobility in a cytophorimeter, expressed as a percentage of the mobility of control cells, for different durations of pronase pretreatment.

previously reported for such cells [21]. The cells in Fig. 2(i)b had been pretreated with pronase (PR = 55%) prior to exposure to dextran. Intercellular spaces with a length in excess of 2 μm can be resolved. When the duration of pronase pretreatment was extended (PR = 47%) a regular periodicity of cell-cell contact points with a reduced lateral separation distance could be discerned (Fig. 2(i)c,d). The sinusoidal outline of the opposite faces of cells in contact in Figs. 2(i)b–d was not detectable in the non pronase-pretreated control cells of Fig. 2(i)a or in cells which had been preincubated for 1 h in PBS/BSA prior to exposure to 2% dextran for 30 min. The second row of Fig. 2 shows pronase pretreated cells (PR = 47%) which had not been fixed before light microscopy. The periodic patterns are also detected and are similar to those seen in cells exposed to 5 μg/ml polylysine (275 kDa) which were photographed without fixation row (iii), Fig. 2). Fig. 2 rows (ii) and (iii) show that the patterns examined in detail by electron microscopy, below for dextran treated cells and elsewhere for polylysine treated cells [15,16], are not artifacts of glutaraldehyde fixation.

The transmission electron micrographs of Fig. 3 contrast low magnification fields of view of (a) non pretreated and (b) pronase pretreated (PR = 47%) cells exposed to dextran. The figure emphasises that parallel contact surfaces are a feature of all of the control clumps and that spatially periodic contact regions are a feature of all clumps of pronase pretreated cells.

Fig. 2 (row (i)) reflects the fact that the lateral separation of contact regions of cells exposed to dextran for equal (30 min) times was shorter for more drastic pronase pretreatments. Fig. 4 shows the average spatial periodicity calculated from measurements of rows of intercellular spaces from at least seven contact seams in representative electron micrographs of cells which had been pretreated, to different extents, with pronase. The

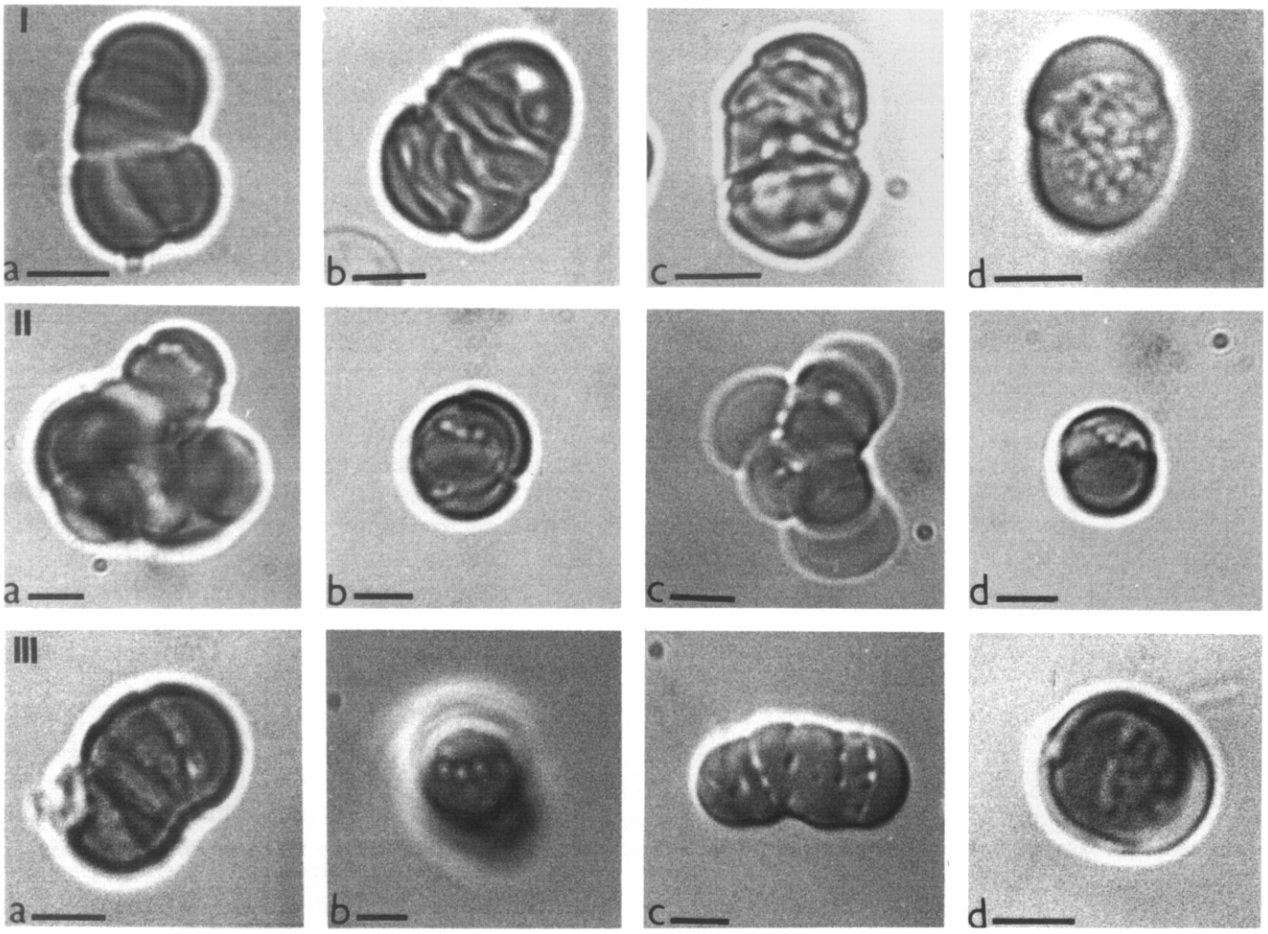

Fig. 2. Light micrographs of erythrocytes exposed: (Row i) to 2% dextran for 30 min at room temperature; (a) normal erythrocytes; (b,c,d) erythrocytes pretreated with 0.5 mg/ml pronase (initial concentration) for 5, 25 and 25 min, respectively. Rows ii and iii show, respectively, examples of unfixed pronase pretreated erythrocytes (0.5 mg/ml pronase for 25 min) exposed to 2% dextran and normal erythrocytes exposed to polylysine (M_r 275000, 5 μg/ml). Bar represents 5 μm.

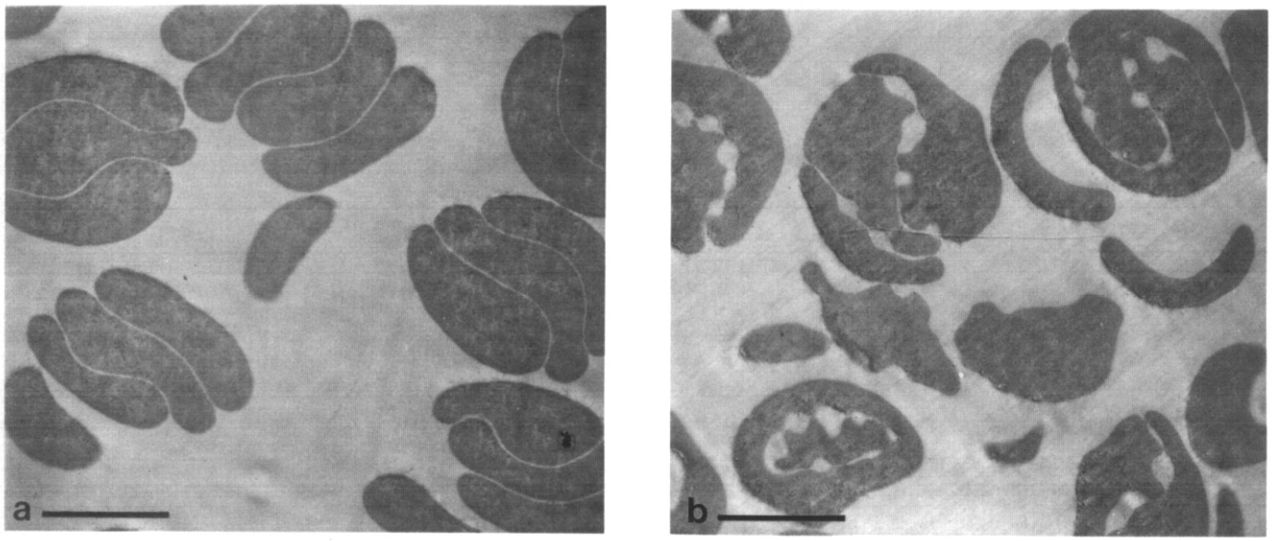

Fig. 3. Transmission electron micrographs of erythrocytes exposed to 2% dextran for 30 min at room temperature: (a) normal cells; (b) cells pretreated with 0.5 mg/ml pronase for 25 min (PR = 47%). Bar represents 5 μm.

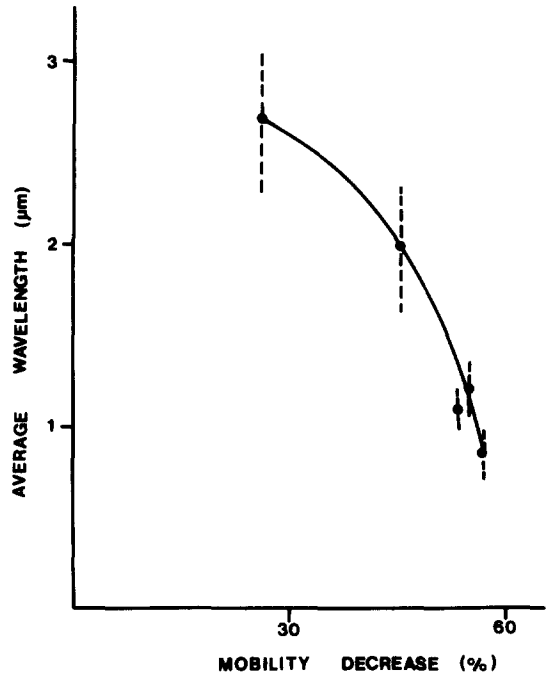

Fig. 4. Average spatial periodicity against percentage decrease in electrophoretic mobility. The average distances between the points of contact were calculated from transmission electron micrographs (95% confidence limits are also shown).

measurements were made on rows containing two or three spaces (three or four contacts) for the longer separations (PR = 73%) and on rows of at least four spacings for the more drastic pronase pretreatments. The measurements from thin section electron micrographs give information, in only one dimension, on separation of contacts distributed over a two-dimensional surface. The calculation of average separations for the different pronase pretreatments was intended to detect consistent differences in spacings for the different pronase pretreatments. The error bars of Fig. 4 include the contributions to variation in average contact separation occurring between different seams and the variation of contact separation along a single seam. The main result is that the average contact separation distance changes significantly with pronase pretreatment.

The high magnification transmission electron micrographs of Fig. 5 show the contact regions resulting from exposure of cells to 2% dextran following different pronase pretreatments. Fig. 5a shows the parallel membranes of non-pretreated erythrocytes when exposed to dextran. A sequence of increasing magnification of the seams of the agglutinate shows that there is no evidence for the occurrence of spatially periodic points of contact. Fig. 5 (rows b–e) shows specific examples of the decrease (from about 3.0 μm to 0.8 μm) in lateral contact separation as the extent of pronase pretreatment was increased. Untreated (no pronase) cells which had been held in PBS/BSA at room temperature for 2 h prior to exposure to 2% dextran showed normal biconcave discoid morphology. Pronase treated cells which were washed and resuspended in PBS/BSA also showed normal morphology.

TABLE I

Real time observation of the adhesion of control cells and pronase pretreated cells (PR = 47%) was monitored by video microscopy. Initial edge-edge contact between two cells was followed after a delay (column 2) by a rapid movement of mutual cell engulfment (column 3).

Cells	Pre-engulfment contact duration (s) (±95% confidence limits)	Engulfment time (s) (±95% confidence limits)
Control	35.1 (±12.9)	0.66 (±0.05)
Pronase treated	18.3 (± 5.97)	0.48 (± 0.1)

Light microscopy showed adhesion patterns as in Fig. 2 with pronase pretreatment dependencies consistent with Figs. 2–5 for as many as 20 different series of experiments (70 pronase pretreatments).

It has been shown [21] that when cells come together in suspension in a microcapillary initial contact occurs at the cell edge and then (after a pause of a number of seconds) the cells undergo a rapid process of mutual engulfment to form a spherical doublet. The cell adhesion has been monitored by video microscopy in the present work for control cells in dextran and for pronase pretreated cells (PR = 47%) in dextran. Table I shows a significant decrease in pre-engulfment delay time and a relatively small decrease in the duration of the engulfment phase for pronase pretreated compared with control cells. It was also noticed that for many of the pronase pretreated cells the initial movement of the rapid engulfment stage was 'signalled' by a slow but noticeable pre-engulfment movement of 0.12 s duration. This short time was not included in the engulfment time in Table I.

Discussion

The above results (Figs. 1(i)a and 5a) show that the cell surfaces within aggregates of dextran-treated normal erythrocytes are uniformly separated, i.e., the membranes of opposite cells remain parallel. This result is consistent with the classical equilibrium DLVO approach [7] to contact of colloidal particles. The parallel surface result is similar to previous results of electron microscopic examination of the contact seam of erythrocytes treated with 3 and 4% solutions of lower (75000) molecular weight dextran [18,19].

The present work shows that, for large (450000) molecular weight dextran, pronase pretreatment of cells leads to a patterned form of contact. These latter results classify contact in pronase-pretreated dextran treated cells with polycation [15,16] and wheat germ agglutinin induced [17] erythrocyte contact. However, the strong

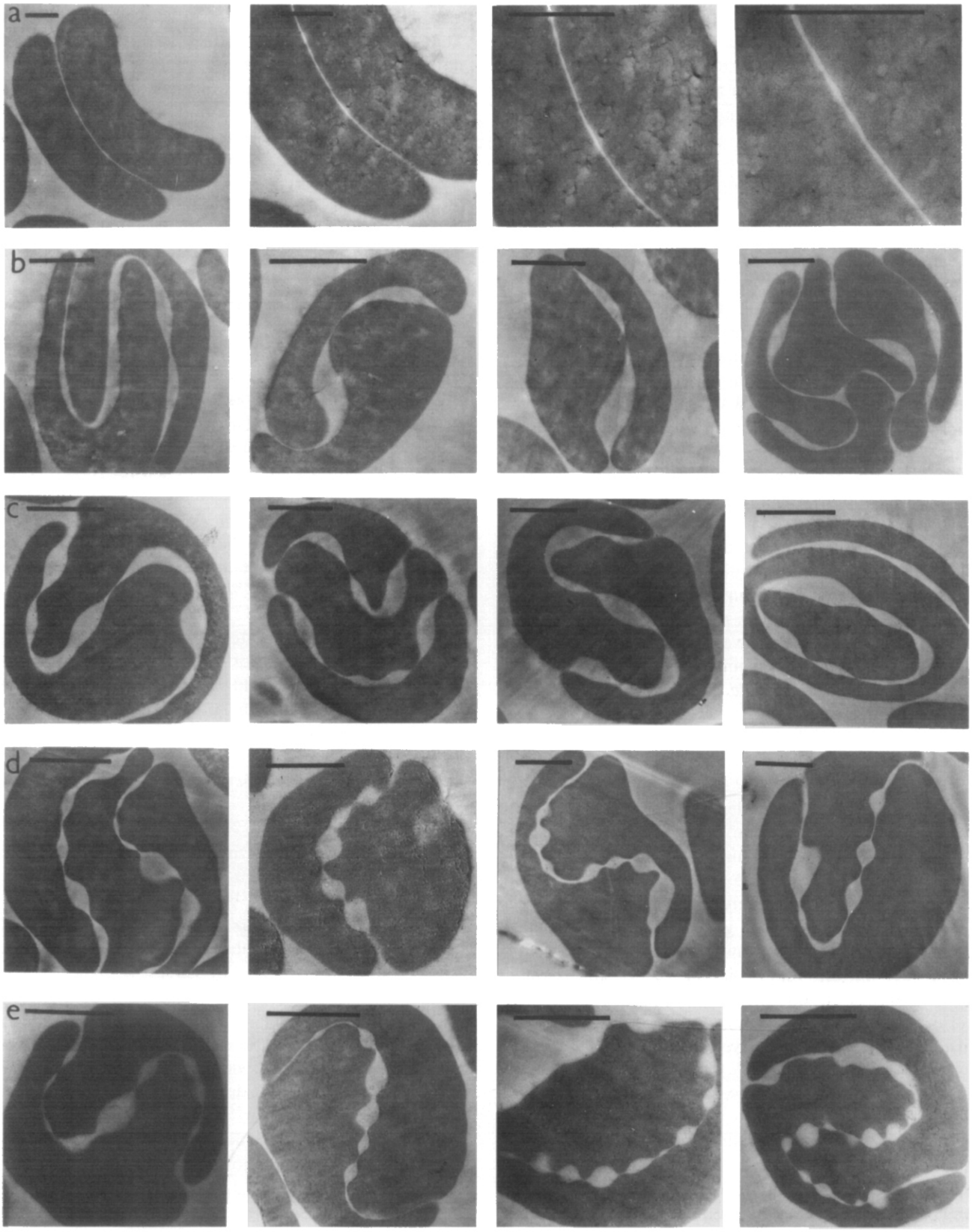

Fig. 5. Transmission electron microscopy of erythrocytes exposed to 2% dextran: Row (a) control cells showing, at different magnifications, the continuous parallel-seam between membranes in a clump. Bar represents 1 μm. Rows (b – e) show examples of erythrocytes pretreated with 0.5 mg/ml pronase for 0.5–1.0 min (PR = 73%), 5 min (PR = 54%), 25 min (PR = 47%), and 2 h (PR = 44%), respectively. Bar represents 2 μm.

dependence of lateral separation of dextran-induced contacts in pronase-pretreated cells on experimental conditions (Fig. 4) contrasts with the situation for polycation and lectin induced point contacts where separation was always close to 0.8 μm [15–17].

The instability criterion for a non-thinning fluid layer (phase 2) between two continuous phases (1 and 3) is given [12] by

$$k^2\sigma_t + k^4B - d\Pi_t/dh < 0 \quad (1)$$

where (a); $k = 2\pi/\lambda$ (λ is the wavelength of the disturbance which will grow to rupture the thin film); the total surface tension $\sigma_t = 2\sigma_s + \sigma_a + \sigma_r$ where σ_s is the pure surface tension of the thin film σ_a and σ_r are contributions to the surface tension from sources of attractive and repulsive interactions, respectively. Contributions to σ_a include terms related to the long range component of the van der Waals interaction, attractive macromolecular crosslinking, and hydrophobic interactions. Contributions to σ_r include hydration effects, stereorepulsion and electrostatic interactions [12]. The membrane bending elastic modulus is $B = 1.8 \cdot 10^{-19}$ J [23]: and

(b); $d\Pi_t/dh$ is the first derivative, with respect to film thickness h, of the net disjoining pressure (i.e., the sum of the attractive and repulsive normal interaction pressures). The second term of the instability criterion above is the second derivative of the interaction potential profile between two membranes. A number of the interaction pressures can be expressed in the general form

$$P(h) = P \cdot \exp(-h/L) \quad (2)$$

where L is a characteristic length and P is a constant. Interactions for which Eqn. 2 is taken to hold are hydration forces ($L \approx 0.3$ nm, [24]; including hydrophobic effects with $L \approx 1.5$ nm [5]), electrostatic (in physiological salt, at relatively large separation; $L \approx 0.4$ nm (half the Debye length)) glycocalyx stereo-repulsion ($L \approx 5$–10 nm; [6,12]), and macromolecular crosslinking ($L \approx 4$ nm for 14000 M_r polylysine [6] and $L > 100$ nm for 500000 M_r dextran [25]).

For the above interactions the contribution to the third term of Eqn. 1 will have the form

$$d\Pi/dh = -P \cdot \exp(-h/L)/L \quad (3)$$

When $L \ll h$ the exponential term of Eqn. 3 will cause the contribution of short range forces to be negligible and the instability condition will depend on the longer range forces. If the system is stable for large h the shorter range forces will become dominant at small separations and may be capable of destabilising the thin layer at low h.

Eqn. 1 applies to thin aqueous films containing surfactant [10]. Dimitrov has pointed out that films with surfactant share properties of membrane bound films in that (i) the surfactant interface is essentially immobile tangentially and (ii) the tension in surfactant and membrane boundaries depends on area change, unlike the case for a pure liquid. It is therefore not unreasonable to use Eqn. 1 as a guide to the stability of a membrane-bound thin film.

The rate of growth of a disturbance on an unstable intermembrane aqueous layer is given [1,12] by

$$w = k^2h^3(2d\pi_t/dh - k^2\sigma_t - k^4B)/24\mu \quad (4)$$

where μ is the viscosity of the dextran solution ($\mu = 2$ mN $\cdot$ s $\cdot$ m^{-2}).

For a wavelength of 3 μm in the present work the third term within parentheses in Eqn. 4 is $3 \cdot 10^6$ N $\cdot$ m^{-3}. An estimate of w can be obtained by taking the surface tension term in Eqn. 4 as zero (see, for example, Ref. 26) and considering only the influence of the bending modulus. Setting, from Eqn. 4, $dw/dk = 0$ gives an expression for the dominant (fastest growing) disturbance wavelength [12]. For this condition it can be shown that $2d\Pi_t/dh$ in Eqn. 4 is three times the value of k^4B, so we have an estimate of the term within the parentheses of Eqn. 4. When $\lambda = 3$ μm, $h \approx 200$ nm (Fig. 5b) and $\mu = 2$ mN $\cdot$ s $\cdot$ m^{-2} then $w \approx 4$ s^{-1}. This value for the growth rate is faster than the measured time (480 ms, Table I) for cells to come together. For a wavelength of 0.8 μm and $h \approx 60$ μm (Fig. 5d) $w = 900$ s^{-1}. Where, in addition to B, we need to consider positive values of σ_t then the corresponding values of w will be greater than those calculated above for the bending modulus case. For the second term in parentheses in Eqn. 4 to be of equal significance to the third term σ_t should be of the order of 10^{-3} mN $\cdot$ m^{-1}.

Fig. 5 suggests that membranes are further apart when the 3 μm wavelength disturbance begins its exponential growth (Fig. 5b) than when the 0.8 μm disturbance (Fig. 5e) grows, i.e., the more drastic pronase pretreatment of the membranes appears to maintain the intercellular water stable at values of h which would lead to disturbance growth for milder pronase pretreatments. This stabilising effect needs to act at relatively large separations, so it is unlikely to be associated with any effects with a small value of L. One possible source of stability would be a decreased negative electrostatic contribution to the surface tension term in Eqn. 1, because of pronase induced surface charge depletion. The negative surface potential contribution to σ_t is given (in c.g.s. units, [10,12]) by

$$\sigma_{dl} = -\varepsilon\kappa\,\phi_s^2 \cdot [(\sinh(\kappa h) - \kappa h)/4\,(\cosh(\kappa h) + 1)] \quad (5)$$

where, for erythrocytes in 145 mM saline, κ^{-1} is 0.8

nm, the surface potential $\sigma_s = 15$ mV, and the dielectric constant ε is 80. The expression within square parentheses grows rapidly to $1/4\ \pi$ as h increases to 10 nm. For values of h in excess of 10 nm σ_{dl} is essentially constant at -0.2 mN/m. Eliminating this negative contribution to σ_t would result in an increase in σ_t and an increase in the value of $k^2\sigma_t$ which would need to be overcome, at large separations, by the long range attractive interaction contributions to $d\Pi_t/dh$ to give a positive growth rate in Eqn. 4. When the wavelength is 1 μm the increase in $k^2\sigma_t$ due to elimination of the σ_{dl} contribution is $8 \cdot 10^9$ N $\cdot$ m^{-3} which is, for instance, greater than the $3 \cdot 10^8$ N $\cdot$ m^{-3} stabilising effect of the bending elasticity term. It can be shown that the destabilising contribution of charge depletion to $d\Pi_t/dh$ will be equal to the stabilising contribution of charge depletion to the second term in Eqn. 5 only when h falls to 10 nm [6]. Because of reduced electrostatic repulsion, reduced glycalyx stereorepulsion and enhanced hydrophobic attraction [27] in pronase-treated cells it is more likely that macromolecular interactions will crosslink the crests of the disturbance to give the periodic contact patterns reported above. It may well be that the drawing together of non-pronase treated cells in dextran also involves fluctuation growth but that the crests of the disturbances are influenced by the electrostatic, stereopulsion, and hydration repulsion forces at small distances of separation. They fail to develop close contact and spreading of the contact region occurs to give parallel membrane apposition in a DLVO secondary minimum [28].

A regular periodicity of protrusions on the cell surface (echinocyte morphology) is seen in erythrocytes when the cells are exposed to a range of environments, e.g., one containing anionic amphipathic drugs [30] or one of alkaline pH [31]. The periodicity shown in the micrographs of Fig. 5 differs from echinocyte formation in that (i) the latter gives protrusions all over the cell surface while the present periodicity is confined to regions of membrane apposition and (ii) environments causing echinocyte formation act on single cells while single cells in the present work have normal morphology; the periodicity is seen only where cells are close together, i.e., it requires membrane–membrane interaction.

It can reasonably be expected that the different outcomes of membrane interaction (i.e., parallel separated membranes or membranes in close spatially periodic contact) have physiological implications. For instance, the sudden contact of the apposing faces of the acrosome outer membrane and the plasma membrane of boar spermatozoa during the acrosome reaction leads to the production of a sheet of essentially equally sized hybrid vesicles consisting of hemispheres of both membranes [32]. Vesiculation of sea urchin sperm head membrane occurs within 1 s of initiation of the acrosome reaction [33]. In another instance, the locomotion of the small amoeba *Naegleria gruberi* over a glass substratum, interference reflection microscopy shows point 'focal' cell-substratum development. The focal points emerge from broad regions (occupying about 1/3 of the cell cross-sectional area) of 'associated contact' between the cell and glass. The focal contacts act to stabilise the associated contact area otherwise undulation of the membrane causes the location of the associated contact to change faster than the resolution (2 s) of the recording system. The 'associated contact'-glass separation depends strongly (110 nm in distilled water, 20 nm in 3 mM NaCl) on ionic strength [33]. The average spacing between focal contact points was 2.4 μm and 1.0 μm when the cell-substratum separation fell from 100 nm to less than 20 μm [34]. This biological example of membrane undulation and of the dependence of membrane-substratum separation and point contact separation on the electrolytic composition of the suspending phase might usefully be examined from the viewpoint of thin film stability.

The experimental results in the present paper provide evidence of an ability to control, by modifying the properties of the interacting membranes, the outcome of a membrane interaction to give either parallel membranes or membranes interacting closely in a spatially periodic pattern.

Acknowledgement

H.D. is supported by a SERC research studentship.

References

1 Dimitrov, D.S. (1982) Colloid Polym. Sci. 260, 1137–1144.
2 Manev, E., Scheludko, A. and Exerova, D. (1974) Colloid Polym. Sci. 252, 586.
3 Jain, R.K., Ivanov, I.B., Jain, R.K. and Ruckenstein, E. (1979) in Dynamics and Instability of Fluid Interfaces (Sorensen, T.S., ed.), pp. 140–167, Springer, Berlin.
4 Radoev, B.P., Scheludko, A.D. and Manen, E.D. (1983) J. Colloid Interface Sci. 95, 254–265.
5 Israelachvili, J.N. and McGuiggan, P.M. (1988) Science 241, 795–800.
6 Coakley, W.T. and Gallez, D. (1989) Biosci. Rep., in press.
7 Hiemenz, P.C. (1985) Principles of Colloid and Surface Chemistry, Marcel Dekker, New York.
8 Dimitrov, D.S. and Jain, R.K. (1984) Biochim. Biophys. Acta 779, 437–468.
9 Prevost, M., Gallez, D. and Sanfeld, A. (1983) J. Chem. Soc. Faraday Trans. II 79, 961–976.
10 Prevost, M. and Gallez, D. (1984) J. Chem. Soc. Faraday Trans. II 80, 517–533.
11 Gallez, D., Prevost, M. and Sanfeld, A. (1984) Colloids Surfaces 10, 123–131.
12 Gallez, D. and Coakley, W.T. (1986) Prog. Biophys. Mol. Biol. 48, 155–199.
13 Fisher, L.R., Parker, N.S. and Haydon, D.A. (1986) Faraday Discuss. Chem. Soc. 81, 249–256.
14 Dimitrov, D.S. (1986) Faraday Discuss. Chem. Soc. 81, 264–265.

15 Coakley, W.T., Hewison, L.A. and Tilley, D. (1985) Eur. Biophys. J. 13, 123–130.
16 Hewison, L.A., Coakley, W.T. and Meyer, H.W. (1988) Cell Biophys. 13, 151–157.
17 Darmani, H., Coakley, W.T., Hann, A.C. and Brain, A. (1990) Cell Biophys. in press.
18 Jan, K.M. and Chien, S. (1973) J. Gen. Physiology 61, 638–654.
19 Skalak, R., Zarda, P.R., Jan, K.M. and Chien, S. (1981) Biophys. J. 35, 771–781.
20 Coakley, W.T., Darmani, H., Irwin, S.A., Robson, K. and Gallez, D. (1988) Stud. Biophys. 127, 69–74.
21 Tilley, D., Coakley, W.T., Gould, R.K., Payne, S. and Hewison, L.A. (1987) Eur. Biophys. J. 14, 499–507.
22 Seaman, C.V.F. (1975) in The Red Blood Cell (Surgeoner, D.M., ed.), Vol. 2, pp. 1135–1229. Academic Press, New York.
23 Evans, E.A. (1983) Biophys. J. 43, 27–30.
24 Rand, R.P., Fuller, N., Parsegian, V.A. and Rau, D.C. (1988) Biochemistry 27, 7711–7722.
25 Edberg, S.C., Bronson, P.M. and Van Oss, C.J. (1972) Immunochemistry 9, 273–281.
26 Fricke, K. and Sackmann, E. (1984) Biochim. Biophys. Acta 803, 145–152.
27 Van Oss, C.J., Gillman, C.F. and Neumann, A.W. (1975) Phagocytic Engulfment and Cell Adhesiveness, pp. 108–131, Dekker, New York.
28 Verwey, E.J.W. and Overbeek, J.Th.G. (1949) Theory of The Stability of Lyophobic Colloids, Elsevier, Amsterdam.
29 Dimitrov, D.S. (1986) Proc. 8th School on Biophysics of Membrane Transport, Vol. 1, Mierki, Poland, pp. 51–82.
30 Nwafor, A. and Coakley, W.T. (1985) Biochem. Pharmacol. 34, 3329–3336.
31 Glaser, R. (1982) J. Membr. Biol. 66, 79–85.
32 Russel, L., Peterson, R. and Freud, M. (1979) J. Exp. Zool. 208, 41–56.
33 Preston, T.M. and King, C.A. (1978) J. Cell Sci. 34, 145–158.
34 King, C.A., Cooper, L. and Preston, T.M. (1983) Protoplasma 118, 10–18.
35 Tilney, L.G. (1985) in Biology of Fertilisation, Vol. 2, pp. 158–213, Academic Press, New York.